LANGMUIR

pubs.acs.org/Langmuir Article

Theory of Charge Regulation of Colloidal Particles in Electrolyte Solutions

Amin Bakhshandeh,* Derek Frydel,* and Yan Levin*

Cite This: *Langmuir* 2022, 38, 13963−13971 Read Online

ACCESS | Metrics & More | Article Recommendations

ABSTRACT: We present a theory that enables us to (i) calculate the effective surface charge of colloidal particles and (ii) efficiently obtain titration curves for different salt concentrations. The theory accounts for the shift of pH of solution due to the presence of 1:1 electrolyte. It also accounts self-consistently for the electrostatic potential produced by the deprotonated surface groups. To examine the accuracy of the theory, we have performed extensive reactive Monte Carlo simulations, which show excellent agreement between theory and simulations without any adjustable parameters.

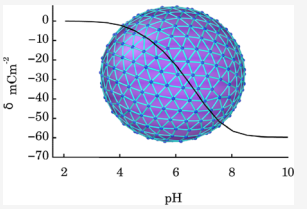

Downloaded via UNIV FED DO RIO GRANDE DO SUL on March 31, 2023 at 16:04:59 (UTC).
See https://pubs.acs.org/sharingguidelines for options on how to legitimately share published articles.

INTRODUCTION

Colloidal particles are important for various applications in chemistry, biology, and physics.[1−5] The vast variety of applications of colloidal systems has made modern society very dependent on these complex systems.[6−10] To stabilize colloidal suspensions, the particles are often synthesized with acidic or basic surface groups. In aqueous suspensions, these groups become ionized, which leads to the formation of electrical double layers (EDLs).[11−19] The complicated physics of EDLs is responsible for the stability of colloidal suspensions and can lead to some very counterintuitive effects, such as reversal of electroscopic mobility in suspensions with multivalent counterions or like-charge attraction between colloidal particles with the same sign of charge.[20−23] The stability of colloidal systems is usually explored using ideas first introduced by Derjaguin, Landau, Verwey, and Overbeek (DLVO) theory.[24−27] However, DLVO theory does not take into account electrostatic correlations[2] between ions and between ions and sites. Such effects can become very important for suspensions containing multivalent counterions and also in suspensions containing large concentrations of 1:1 electrolyte. Furthermore, the charge of colloidal particles is not constant, but is dependent on the pH and electrolyte concentration inside the suspension. The fluctuation of colloidal charge can lead to some very nontrivial effects, in particular, those close to the isoelectric point.[28] The process of charging the colloidal particles is denoted as "charge regulation" (CR) and was first elucidated by Linderstrøm-Lang.[29] The first quantitative model of CR was proposed by Ninham and Parsegian.[30] The NP approach is based on Poisson−Boltzmann (PB) theory, which neglects the discrete nature of colloidal surface groups and electrostatic correlation effects.[31−37] Indeed, PB theory is known to be very accurate for suspensions with monovalent 1:1 electrolytes. However, recent works, based on Baxter's model of sticky spheres to describe protonation/deprotonation equilibrium, showed[38−41] that discreteness of surface groups significantly affects the effective charge predicted by the NP theory. The importance of ion polarizability and of finite ion size was also explored in ref 42.

The Baxter model of protonation also showed that there is a change in equilibrium constant when an acidic group is moved from bulk to the surface.[38−41] Generally, the renormalization of the equilibrium constant is due to the broken rotational and translational symmetry at the surface, compared to the bulk. However, the theory developed showed that both the discrete charge effects and the renormalization of the bulk equilibrium constant by the surface can be included within the NP framework. However, the calculations were not entirely self-consistent, since the discreteness effects were not taken into account at the same level of mean-field approximation as are implicit in the PB equation. In the present work, we correct this omission and also account for the shift in pH produced by the dissolved electrolyte. Both of these effects become important for suspensions with weak acidic surface groups in suspensions with salt.

The rest of the paper is organized as follows: in the section entitled "Theory", we present the fully self-consistent theory of charge regulation. In the section entitled "Reactive Monte Carlo Simulations", we briefly describe the simulation method used to compare with the predictions of the theory. In section entitled "Transcendental Approximation", we present a simple transcendental equation that provides us with an easy way of calculating the effective colloidal charge and titration curves in

Received: August 25, 2022
Revised: October 7, 2022
Published: November 1, 2022

ACS Publications © 2022 American Chemical Society

https://doi.org/10.1021/acs.langmuir.2c02313
Langmuir 2022, 38, 13963−13971

suspensions at large dilution. Finally, in the last section, we present the conclusions of the present work.

THEORY

We study a colloidal particle of radius a, containing Z acidic surface groups. The particle is confined inside a spherical Wigner−Seitz (WS) cell of radius R, which is determined by the concentration γ of colloidal suspension ($\gamma = (3/4)\pi R^3$). The suspension is in contact with a reservoir of salt and acid at bakhshandehconcentrations c_s and c_a, respectively. For reader's convenience, in Table 1, we present a list of symbols that appear in the rest of the paper.

Table 1. Symbols/Variables Used in the Rest of the Paper

symbol	significance
λ_B= 7.2 Å	Bjerrum length
β	$1/k_BT$
f_0	free energy of a deprotonated state of a site
f_1	free energy of a protonated state of a site
μ	chemical potential
K	equilibrium constant
Λ	de Broglie thermal wavelength
c_i	concentration of electrolyte
a_i	activity of electrolyte
ϕ_s	isolated site electrostatic potential
ϕ	mean-field electrostatic potential
κ	Debye length
M = 1.106	Madelung constant
ϵ_w	dielectric constant of water
a	colloidal radius
γ	colloidal volume fraction
R	cell size
Z_{eff}	number of deprotonated groups
$K_a = 1/K$	acid dissociation constant
q	proton charge
$\varphi(\mathbf{r})$	electrostatic potential at position $\mathbf{r}$
Q	colloidal charge
σ	surface charge density
ξ	probability of deprotonation of surface group

The number of deprotonated surface groups Z_{eff} is determined by the chemothermodynamic equilibrium. The charge of the colloidal particle can then be written as $Q = -Z_{\text{eff}}q = -Zq\xi$, where q is the proton charge and ξ is the probability that a surface group is deprotonated:

$$\xi = \frac{\exp(-\beta f_0)}{\exp(-\beta f_0) + \exp(-\beta f_1)} \tag{1}$$

In this expression, f_0 is the free energy of a deprotonated state and f_1 is the free energy of a protonated state of a site. f_0 is due to electrostatic free energy of solvation of a surface group inside an electrolyte solution, $f_0 = \mu_{\text{solv}}$. The ions of electrolyte partially screen the electric field produced by a surface group lowering its overall electrostatic self-energy. Dividing the numerator and denominator of eq 1 by $\exp(-\beta f_0)$, we can write

$$Z_{\text{eff}} = \frac{Z}{1 + \exp(-\beta\Delta\mu)} \tag{2}$$

where $\Delta\mu = f_1 - f_0$ is the difference in free energy between protonated and deprotonated states of surface active groups. We should note that Z_{eff} should not be confused with the far field effective charge often defined in studies of colloidal systems[2,43,44]

Consider a reaction occurring on the colloidal surface:

$$H^+ + A^- \rightleftharpoons HA \tag{3}$$

where A^- is a surface deprotonated group and K is the equilibrium constant of the reaction. The equilibrium constant K is related to the weak acid dissociation constant by $K = 1/K_a$. As discussed in the Introduction, the value of surface K is generally different from the same reaction occurring in the bulk. K accounts for the direct electrostatic interaction of proton with an isolated surface group bound to the surface. This can only be calculated using quantum density functional theory. At the semiclassical level, we can denote $\zeta = K/\Lambda_{H^+}^3$—where Λ_{H^+} is the proton de Broglie thermal wavelength—as the internal partition function for a HA "surface molecule". In addition to this interaction, when the proton is moved from the reservoir to the colloidal surface, it will also interact with the other surface groups. Since, these groups are reasonably far away, the quantum effects can be neglected and the long-range interaction can be modeled using classical electrostatics. The change in free energy due to removal of a hydronium ion from the reservoir and transferring it to colloidal surface, where the following reaction then occurs:

$$\beta\Delta\mu = -\ln\left(\frac{K}{\Lambda_{H^+}^3}\right) + \beta q\varphi - \beta\mu_{\text{solv}} - \ln(c_a\Lambda_{H^+}^3) - \beta\mu_{\text{ex}} \tag{4}$$

The first term on the right-hand side of this expression is the free energy of direct interaction of proton with the adsorption site, the second term is the mean electrostatic energy of proton interacting with all the other deprotonated acid groups and with the ions of solution. The third term is the loss of electrostatic solvation free energy when the site becomes protonated (neutral). Finally, the last two terms are the free-energy change of the reservoir when one hydronium ion is moved to the colloidal surface. The excess chemical potential μ_{ex} is an important part of the proton activity, $a_{H^+} = c_a e^{\beta\mu^{ex}}/c_a^\circ$, where c_a° = 1 M is the standard reference concentration. The pH of a suspension containing electrolyte is defined as pH = $-\log_{10}[a_{H^+}]$. For 1:1 electrolyte μ_{ex} is very accurately accounted for using the mean spherical (MSA)[45] and Carnahan−Starling (CS) approximations, $\mu^{\text{ex}} = \mu_{\text{CS}} + \mu_{\text{MSA}}$, where

$$\beta\mu_{MSA} = \frac{\kappa d\sqrt{1 + 2\kappa d} - \kappa d - (\kappa d)^2}{8\pi c_t d^3} \tag{5}$$

and

$$\beta\mu_{\text{CS}} = \frac{8\eta - 9\eta^2 + 3\eta^3}{(1 - \eta)^3} \tag{6}$$

where d = 4 Å is the ionic diameter, which, for simplicity, we assume to be the same for all ions, κ is the inverse Debye length ($\kappa = =\sqrt{8\pi\lambda_B c_t}$), $c_t = c_a + c_s$, λ_B is the Bjerrum length, which is 7.2 Å in water at room temperature ($\lambda_B = q^2/k_BT\epsilon_w\lambda_B\ \lambda_B$, and $\eta = \left(\frac{\pi d^3}{3}\right)c_t$. Substituting this into eq 2, we obtain

$$Z_{\text{eff}} = \frac{Z}{1 + Kc_a e^{-\beta(\varphi - \mu^{ex} - \mu_{sol})}} \tag{7}$$

Electrostatic Free Energy of Solvation of Surface Site. To calculate the electrostatic solvation free energy of an isolated

https://doi.org/10.1021/acs.langmuir.2c02313
Langmuir 2022, 38, 13963−13971

group of charge q_s located on the surface of a colloidal particle, we neglect the curvature effects and treat the surface as an infinite plane. This is very reasonable for suspensions containing a lot of salt—for which electrostatic solvation energy is significant—since the electrostatic curvature effects will be screened on the scale larger than the Debye length.

We will work in a cylindrical coordinate system, with the colloidal surface located at $z = -h$, where $h = d/2 = r_{ion}$ (see Figure 1). Because of hardcore repulsion between ions and

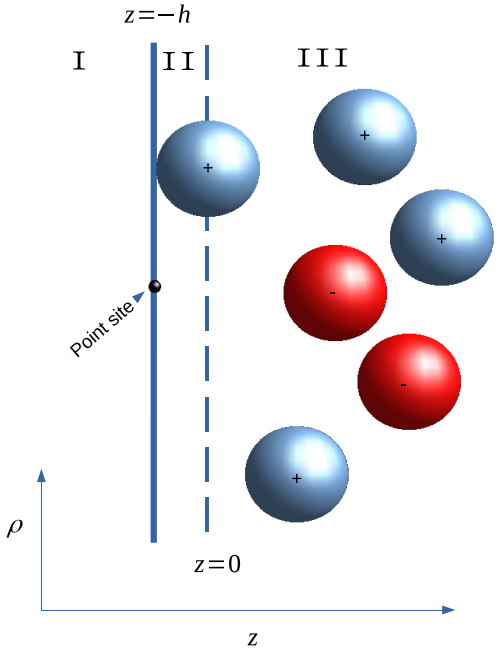

Figure 1. Schematic representation of an isolated adsorption site on colloidal surface, with exclusion zone due to hard core repulsion of ions from the surface.

colloidal surface, we see that there is an exclusion layer where no ions are present. Within the Debye–Hückel approximation, the electrostatic potential then satisfies

$$\begin{cases} \nabla^2 \phi_s(\rho, z) = -2q_s \dfrac{\delta(\rho)\delta(z+h)}{\rho} & z < 0 \\ \nabla^2 \phi_s(\rho, z) = \kappa^2 \phi_s(\rho, z) & z > 0 \end{cases} \tag{8}$$

Using the azimuthal symmetry of the problem, the solution can be written as[46]

$$\phi_s(\rho, z) = \frac{q_s}{2\pi} \int_0^\infty \mathrm{d}k\, k J_0(k\rho) \tilde{\phi}_s(k, z) \tag{9}$$

Substituting this into eqs 8, we obtain

$$\tilde{\phi}_s(k, z) = \frac{2\pi}{k}\left[e^{-k|z+h|} + \frac{k-p}{k+p} e^{k(z-h)} \right] \qquad \text{for } z < 0 \tag{10}$$

where $p = \sqrt{k^2 + \kappa^2}$. Substituting eq 10 back into eq 9, the integral over the first term can be performed analytically, resulting in the usual Coulomb potential produced by the charge q_s located at $(\rho = 0, z = -h)$. Therefore, the second term gives us the induced potential produced by the polarization of the ionic atmosphere by the surface charge group. The electrolyte partially screens the electric field of the charged site, resulting in negative electrostatic solvation free energy, which can be calculated using the Güntelberg charging process.[46,47] We find[48]

$$\beta\mu_{sol} = \frac{\lambda_B}{2} \int_0^\infty \frac{k - \sqrt{\kappa^2 + k^2}}{k + \sqrt{\kappa^2 + k^2}} e^{-2kr_{ion}}\, \mathrm{d}k \tag{11}$$

ELECTROSTATIC POTENTIAL

The electrostatic potential that an adsorbed proton feels can be separated into two contributions: the direct electrostatic interaction with the adsorption site and the interaction with the other sites and with the ions of electrolyte. The direct interaction with the adsorption site is already included inside the $\Delta\mu$ term, through the equilibrium association constant K. The interaction with the other sites and with the ions of electrolyte, φ, can be separated into two contributions by adding and subtracting a uniform neutralizing background, $\varphi = \phi_0 + \phi_{disc}$, where ϕ_0 is the potential produced by the subtracted neutralizing background together with the ions of electrolyte. This potential is very close to the mean surface potential produced by a *uniformly* charged sphere, of charge density $\sigma = -Z_{eff}q/4\pi a^2$, inside an electrolyte solution. The potential ϕ_{disc} is then, the electrostatic potential produced at the position of adsorption site i by the other deprotonated sites and by their neutralizing background.

We will assume that the sites on the surface of colloidal particle have hexagonal order. Strictly speaking, one cannot tile a spherical surface with hexagons, so defects must be present. The defects, however, modify the electrostatic energy only slightly.[49] The optimum distribution of charges on a spherical surface, such that it minimizes the electrostatic Coulomb energy, is a well-studied Thomson ordering problem.[50−53] The electrostatic energy of Z point sites of charge $-q$, arranged with pseudohexagonal Thomson order on a surface of a sphere with a uniform neutralizing background, is very well approximated by[49]

$$E_{dis} \approx \frac{-Mq^2 Z^{3/2}}{2a\epsilon_w} \tag{12}$$

where $M = 1.106$ is the Madelung constant of a planar hexagonal lattice of charges on a neutralizing background. If n of the surface sites are protonated, the mean charge of each surface site is $q(1 - n/Z)$. In equilibrium protons can hop between the sites, so that at the mean-field level of approximation the energy of a Thomson sphere with n neutralized sites is

$$E_{disc}(n) = \frac{-MZ^{3/2}q^2\left(1 - \frac{n}{Z}\right)^2}{2a\epsilon_w} \tag{13}$$

Note that at the mean-field level of approximation, we neglect the correlations between the condensed protons so that their charge is effectively smeared uniformly between the adsorption sites. This is precisely the same level of approximation that is implicit in the Poisson–Boltzmann equation, which also neglects the electrostatic correlations.[2]

The ϕ_{disc} is the change in energy when an additional site becomes protonated ($\Delta n = 1$),

$$\beta\phi_{disc} \approx \frac{\partial E_{disc}}{\partial n} = \frac{\lambda_b M\left(1 - \frac{n}{Z}\right)\sqrt{Z}}{a\epsilon_w} = \frac{\lambda_b M Z_{eff}}{a\epsilon_w\sqrt{Z}} \tag{14}$$

https://doi.org/10.1021/acs.langmuir.2c02313
Langmuir 2022, 38, 13963−13971

The concentration of ions inside a WS cell is determined by the equivalence of electrochemical potentials in the reservoir and in the WS cell:

$$q_i\varphi(\mathbf{r}) + \ln[c_i(\mathbf{r})] + \mu^{ex}(\mathbf{r}) = \ln(c_i^{res}) + \mu^{ex} \quad (15)$$

where $\varphi(\mathbf{r})$ is the electrostatic potential at position $\mathbf{r}$ and c_i is concentration of ion of type i. We will suppose that the excess contribution to the chemical potential in the reservoir and inside the WS are approximately the same and will cancel out. Furthermore, the discreteness effects of the surface groups decay very rapidly away from colloidal surface, so that they can be replaced by a uniform surface charge density, so that $\varphi(\mathbf{r}) = \phi(r)$ for $r > a + r_{ion}$. Combining this with eq 15, we arrive at the usual Poisson−Boltzmann (PB) equation:

$$\nabla^2\phi(r) = \frac{8\pi q}{\epsilon_w}(c_a + c_s)\sinh[\beta\phi(r)] \quad (16)$$

Since the hardcore repulsion will prevent the presence of ions within $a < r < a + r_{ion}$, in this region, the electrostatic potential will satisfy the Laplace equation. To check the validity of our "smearing" approximation in which the discrete surface charge is replaced by a uniform surface charge density $\sigma = -Z_{eff}q/4\pi a^2$ in order to calculate the ionic distribution, we perform a grand canonical Monte Carlo (GCMC) to obtain the ionic density profiles inside the WS cell for a colloidal particle with $Z_{eff} = 600$ charged sites. We then compare this profiles to the ones calculated using eq 16 (see Figure 2).

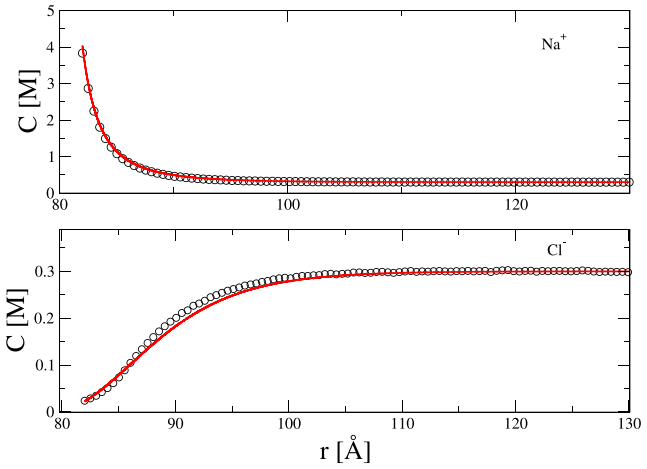

Figure 2. Comparison of ionic density profiles obtained using simulation (symbols) and PB equation for a colloidal particle of radius 80 Å and 600 point charged site randomly distributed on its surface, inside an electrolyte solution of 300 mM.

We see a very good agreement between ionic density profiles calculated using GCMC simulations and PB equation. As can be observed, the discreteness effects are not important away from colloidal surface. The lack of correlational effects on ionic distribution can be partially attributed to the cancellation of the correlational contribution to the electrochemical potential between the reservoir and the system, as discussed following Eq. 15. We can now identify the value of $\phi(a)$ with ϕ_0.

In the calculation above, we have arbitrarily fixed the effective charge; in reality, it must be determined self-consistently using eqs 7 and 16. To solve these equations, we proceed iteratively. We first guess the mean-field potential $\phi(a) = \phi_0$. For this guess, we solve eq 7 to numerically determine the colloidal charge. The Gauss law then provides us with the electric field, or equivalently $\phi'(a) = Z_{eff}q/\epsilon_w a^2$. Using $\phi(a)$ and $\phi'(a)$ as initial conditions, we then integrate the PB equation (eq 16), using the Runge−Kutta fourth-order algorithm. If the electric field at the cell boundary $r = R$, or equivalently $\phi'(R)$, is not zero, as is required by the overall charge neutrality of the system, we adjust our initial guess for ϕ_0. In practice, finding the correct surface potential ϕ_0 is facilitated by combining the algorithm described above with the Newton−Raphson root finding subroutine.

REACTIVE MONTE CARLO SIMULATIONS

There are different simulation methods available to calculate the effective charge in CR systems. To the best of our knowledge, the first Monte Carlo simulation method for titration was introduced by Nishio[54] in 1994. The subsequent research extended this early work to account for the over all charge neutrality inside the simulation cell and for the presence of explicit hydronium ions.[55−61] Here, we will use a reactive Monte Carlo (rMC) simulation method,[62] which is particularly easy to implement for the present colloidal system. Just like in the theory described above, the colloidal particle is located at the center of a Wigner−Seitz (WS) cell, which is in contact with an infinite reservoir of salt and strong acid. The WS cell radius is R = 120 Å (unless specified differently) and the colloidal radius is 80 Å. The intrinsic $pK_a = -\log_{10}K_a = \log_{10}K$ of a functional group on the colloidal surface is taken to be 5.4, similar to that of carboxylic acids. The functional groups are treated as point sites located on the colloidal surface. The reservoir contains strong acid, HCl, and strong electrolyte NaCl, which are assumed to be fully dissociated. A proton associates with water molecule forming a hydronium ion. Again to be consistent with the theory above, we will treat all ions as having the same radius r_{ion} = 2 Å. Water is treated implicitly, with the Bjerrum length set to λ_B = 7.2 Å. The interaction energy between all particles includes the normal Coulomb potential and a hardcore repulsion between ions, colloidal particle, and WS cell boundary.

The simulation consists of standard grand canonical Monte Carlo (GCMC) insertion/deletion moves, as well as protonation and deprotonation moves. The insertion/deletions and protonation/deprotonation moves must always involve a cation−anion pair to preserve the charge neutrality inside the simulation cell. The excess chemical potential μ_{ex} inside the reservoir can be calculated using a separate simulation. This can be done using Widom insertion method in a canonical MC with a fixed concentration of acid and salt in a cubic simulation cell with periodic boundary conditions, or using a reverse GCMC strategy in which the value of μ_{ex} in GCMC is adjusted until the target concentration inside the simulation cell is reached.[62,63] In order to accurately calculate the excess chemical potential for a specific concentration of acid and salt inside an infinite reservoir, it is important to use Ewald summation to treat all the electrostatic interactions between ions.

The acceptance of titration move is given by $acc \rightarrow \min(1, \phi_{p/d})$, where p refers to protonation and d to deprotonation:[62]

$$\phi_p = \frac{c_{H^+}KVc_{Cl^-}}{(N_{Cl^-}+1)}\exp[-\beta(\Delta E_{ele} - \mu_{H^+}^{ex} - \mu_{Cl^-}^{ex})]$$

$$\phi_d = \frac{N_{Cl^-}}{c_{H^+}KVc_{Cl^-}}\exp[-\beta(\Delta E_{ele} + \mu_{H^+}^{ex} + \mu_{Cl^-}^{ex})] \quad (17)$$

where N_{Cl^-}, V, ΔE_{ele} are the number of Cl^- ions, accessible volume of the WS cell, and change in electrostatic energy inside

https://doi.org/10.1021/acs.langmuir.2c02313
Langmuir 2022, 38, 13963−13971

the cell upon a trial move, respectively. It is important to note that titration move is always combined with insertion or deletion of Cl^- to preserve the charge neutrality of the system. See the schematic in Figure 3. The $\mu^{ex}_{H^+}$ and $\mu^{ex}_{Cl^-}$ are the excess chemical

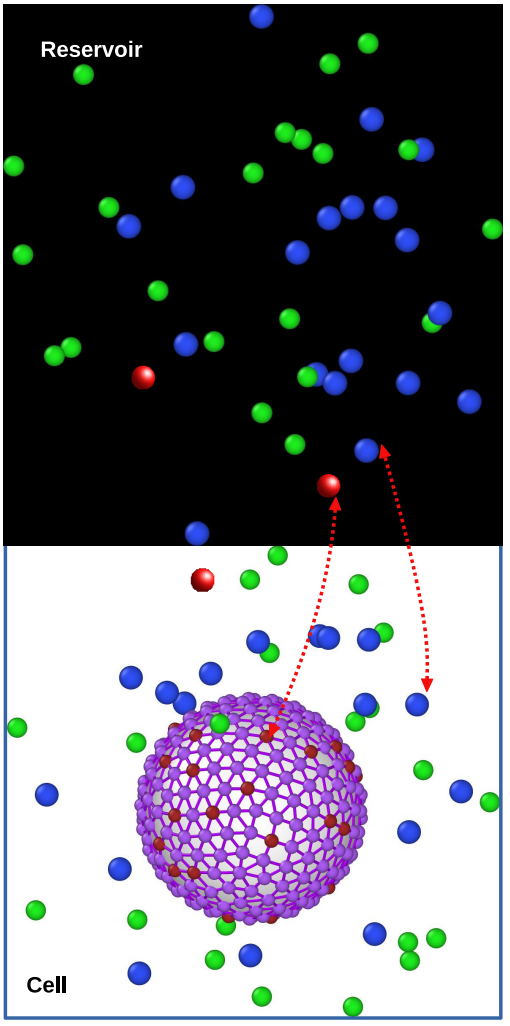

Figure 3. Schematic representation of reactive MC moves. Red, blue, and green spheres are H_3O^+, Cl^-, and Na^+, respectively. The pair H_3O^+ and Cl^- enters the cell from reservoir, H^+ can go to the colloidal surface and react with a site, while Cl^- moves into the bulk with rMC probabilities given by eq 17). Alternatively, H_3O^+ can also move to the bulk. Similarly a pair Na^+ and Cl^- can move between the cell and the reservoir. All the bulk moves are performed with standard GCMC probabilities. All moves are done in pairs to preserve the charge neutrality inside the simulation cell.

potentials of hydronium and of Cl^- in the reservoir. In the present model, with all ions of the same size, $\mu^{ex}_{H^+} = \mu^{ex}_{Cl^-} = \mu^{ex}_{Na^+}$. The same value of $K_a = 1/K = 3.95 \times 10^{-6}$ M, corresponding to carboxylic acid, is used in simulations and in the theory, so that there are no adjustable parameters.

We start by studying the dependence of titration curves on the distribution of surface charge groups. Two possibilities are explored: (1) a random distribution of sites and (2) annealed distribution in which sites are first allowed to arrange on the surface of a sphere, to minimize their repulsive Coulomb energy. This results in Thomson, pseudohexagonal, ordering of sites on colloidal surface. The Thomson configuration of reactive sites is then frozen and rMC is performed. We recall that pH = $-\log_{10} a_{H^+}$, where $a_{H^+} = e^{\beta\mu_{H^+}} = \Lambda^3_{H^+} c^\circ$, so that pH can be written as $pH = -\log_{10}[H^+/c^\circ] - 0.434294\,\beta\mu^{ex}_{H^+}$. In Figure 4, we see that

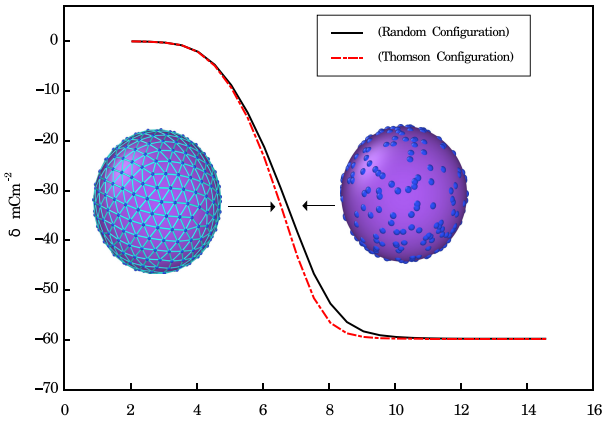

Figure 4. Comparison of titration curves for Thomson and random distributions of surface charge groups.

there is some dependence of titration curves on the distribution of adsorption sites. To be consistent with the theoretical model, and to avoid calculating averages over disorder, in the rest of this paper, we will use a Thomson site distribution.

We now apply the theory developed above to calculate the ionic density profiles around colloidal particle of radius 80 Å with $Z = 600$ carboxyl surface groups, inside suspension containing 300 mM of 1:1 electrolyte for various pH values, see Figure 5. The density of sites on colloidal surface is the same as that found in experimental systems.[64]

We see good agreement between the simulations and the theory. The deviations appear for small pH values, when most of surface groups are protonated and small number of deprotonated groups can not be accurately described by the continuum mean-field theory developed here. Nevertheless, even under these extreme conditions, the agreement between theory and simulations is quite reasonable.

TRANSCENDENTAL APPROXIMATION

Solution of differential eq 16 with charge regulation boundary condition is numerically involved. Often, one does not need the full ionic distribution, but only the effective colloidal charge at very low volume fractions. In this case, the calculation can be significantly simplified by letting the radius of WS become very large, $R \to \infty$. Under these conditions the mean electrostatic potential at contact, ϕ_c, at distance r_{ion} from colloidal surface of a *uniformly* charged particle can be related with the effective charge by[8]

$$Z_{eff} = -\frac{2\kappa(a + r_{ion})^2}{\lambda_B}\left[\sinh\left(\frac{\beta\phi_c}{2}\right) + \frac{2}{\kappa(a + r_{ion})}\tanh\left(\frac{\beta\phi_c}{4}\right)\right] \quad (18)$$

The first term on the right-hand side is the usual relationship between the surface charge density and surface potential for a planar PB equation, while the second term is the leading curvature correction.[8] Within the ion free layer, $a < r < a + r_{ion}$, the mean electrostatic potential is then

https://doi.org/10.1021/acs.langmuir.2c02313
Langmuir 2022, 38, 13963−13971

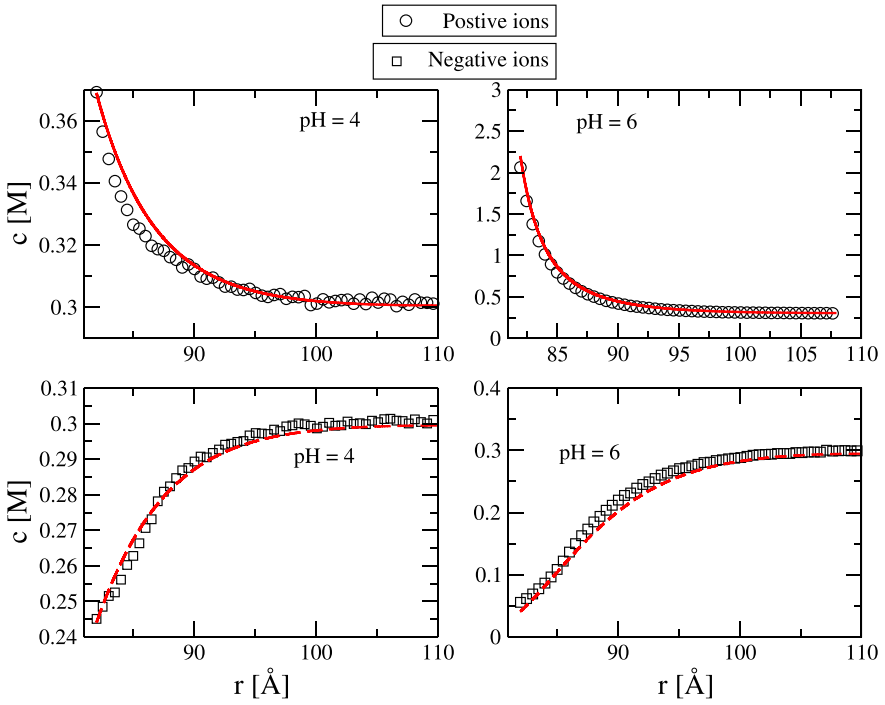

Figure 5. Comparison of ionic density profile for pH 4 and 6 of a colloidal particle with 600 active sites with $K_a = 1/K = 3.95 \times 10^{-6}$ M and radius 80 Å, the concentration of 1:1 salt is 300 mM. Symbols are simulation results and solid curve is the theory.

$$\beta\phi(r) = -Z_{\text{eff}}\lambda_B\left[\frac{1}{r} - \frac{1}{a + r_{\text{ion}}}\right] + \phi_c \tag{19}$$

The electrostatic potential on the surface of colloidal particles with a uniform surface charge density σ is then

$$\beta\phi_0 = \beta\phi(a) = -\frac{Z_{\text{eff}}\lambda_B r_{\text{ion}}}{a(a + r_{\text{ion}})} + \phi_c \tag{20}$$

Substituting eqs 18, 20, and 14 into the charge regulation equation,

$$Z_{\text{eff}} = \frac{Z}{1 + Kc_a e^{-\beta(\phi_0 + \phi_{\text{disc}} - \mu^{\text{ex}} - \mu_{\text{sol}})}} \tag{21}$$

we obtain a self-consistent equation for the contact potential ϕ_c, from which the effective charge can be calculated directly using eq 18. This procedure is much simpler than solving the spherical PB equation with charge regulation boundary conditions. On the other hand, it does not allow us to study the dependence of the effective charge on colloidal concentration or calculate the ionic density profiles. For large WS cells, however, we see an excellent agreement between the colloidal charges calculated using the transcendental approximation and the full theory, see the colloidal charges calculated for a particle of radius 80 Å with surface groups with intrinsic pK_a= 5.4 in a suspension containing 300 mM of 1:1 electrolyte at different pHs, presented in Table 2.

As is demonstrated in Table 2, there is very good agreement between σ obtained using the numerical solution of spherical PB with CR boundary condition and the one calculated using the approximation in eq 18. We can now use the approximation from eq 18 to efficiently calculate the titration curves of colloidal particles in suspensions of low volume fractions. We start with a colloidal particle with $-Zq = -59.6$ mC/m^2 in suspensions with either 10 mM or 300 mM of 1:1 electrolyte (see Figure 6).

Table 2. Comparison of the Surface Charge Density Obtained Using Numerical Solution of the Spherical Nonlinear PB Equation with CR Boundary Condition inside a WS Cell of R = 140 Å with the Transcendental Approximation Method

	Surface Charge Density (mC/m^2)	
pH	full theory	transcendental approximation
4	−6.84	−6.80
5	−33.151	−32.592
6	−80.777	−79.119
7	−112.68	−111.9
8	−118.7	−118.68

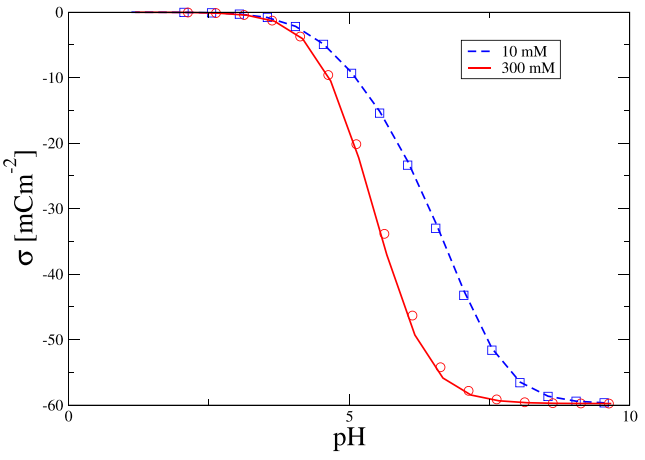

Figure 6. Titration curve for colloidal particle with $-Zq = -59.6$ mC/m^2. The theoretical curves are calculated using transcendental approximation equations. Solid curve is for suspension containing 300 mM salt and the dashed curve is for 10 mM salt solution. The symbols are simulation results.

https://doi.org/10.1021/acs.langmuir.2c02313
Langmuir 2022, 38, 13963−13971

We see an excellent agreement between theory and simulations, without any adjustable parameters. We next study more highly charged particle with $-Zq = -119.4$ mC/m^2; see Figure 7.

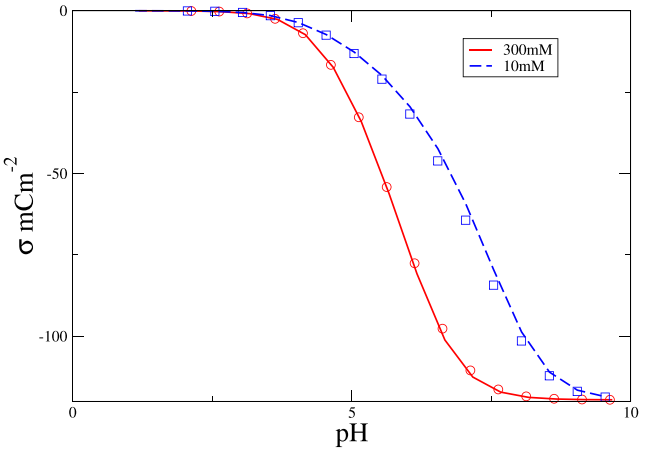

Figure 7. Comparison of titration curve obtained from simulation and theory. The number of acid groups is such that $-Zq = -119.4$ mC/m^2. The solid and dashed line are for the salt concentrations 300 mM and 10 mM, respectively. The symbols represent simulation data points.

Here, once again, theory and simulations show good agreement. The agreement persists even for higher salt concentrations, as can be seen in Figure 8 showing the titration curves for salt concentration of 500 mM and 10 mM of particles with $-Zq = -71.6$ mC/m^2.

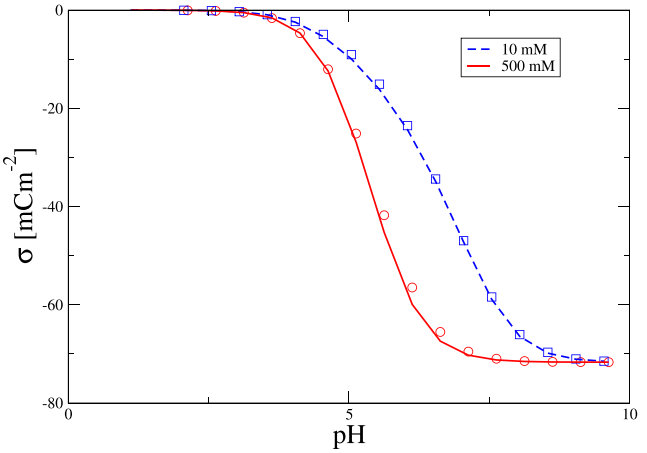

Figure 8. Titration of a colloidal particle with $-Zq = -71.59$ mC/m^2. The solid and dashed line are for the salt concentrations 500 mM and 10 mM, respectively. The symbols represent simulation data and curves represent the theoretical values.

To ensure that the good agreement observed between simulations and theory is not due to the specific value of K_a, we next study colloidal particle with stronger acidic surface groups of $K_a = 8.1 \times 10^{-5}$ M, pK_a 4.09. Furthermore, to clearly see the effect of discreteness of surface charge groups and of electrostatic correlations on CR, in addition to the present theory, we also present the "conventional" titration curves in which these effects are neglected,[54,65] i.e., $\mu^{ex} = \phi_{dis} = \mu_{sol} = 0$. As can be seen from Figure 9, the present theory once again agrees very well with the simulations, while the conventional titration curves show strong deviations.

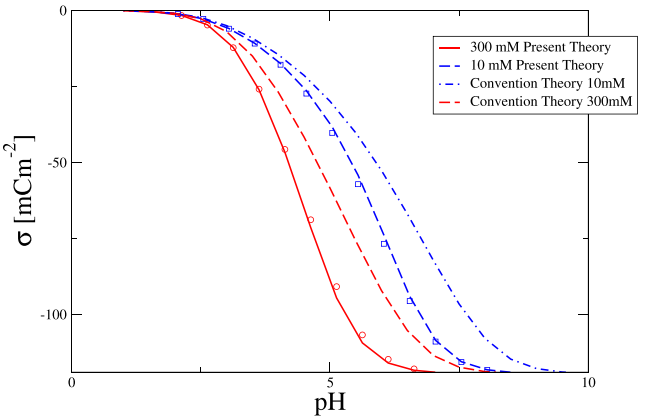

Figure 9. Titration of a colloidal particle of surface charge density -71.6 mC/m^2 with surface groups of intrinsic pK_a = 4.09. The symbols represent simulation data points. The curves correspond to the results of the present theory and to "conventional" titration, in which the discreteness and the correlational effects are neglected.

We next solve the full nonlinear PB equation with our CR boundary conditions to calculate the ionic density profiles around this colloidal particles at pH 6 and 10 mM NaCl. The theory once again shows good agreement with the simulations (see Figure 10). On the other hand, when the discreteness and solvation energies are neglected, one sees strong deviations in ionic density profiles.

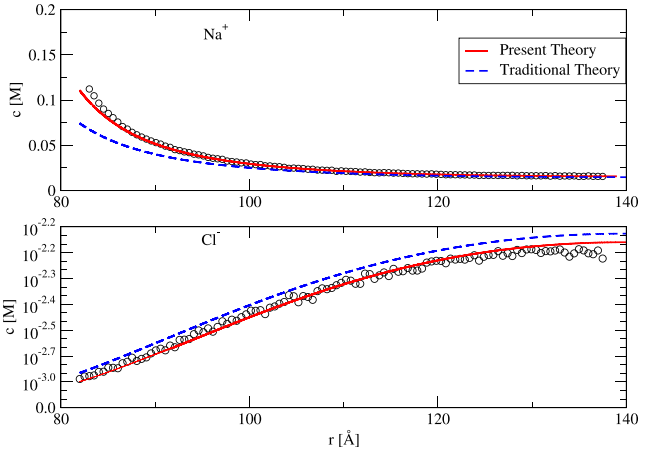

Figure 10. Ionic density profiles around a colloidal particle predicted by the present theory and by the conventional titration model in which discreteness and correlational effects are neglected.

In a recent paper,[59] authors argued that pH − pK_a is a "universal" parameter, namely that one will obtain an identical number of protonated groups for systems with different pH and pK_a, as long as pH − pK_a = constant. Our theory shows that this is not the case, even in the absence of salt. To demonstrate this, we study colloidal particles of radius 103.3 Å with $Z = 600$ surface groups, inside a WS cell of radius 140 Å. The concentration of salt in the reservoir is set to zero. First, we fix the intrinsic pK_a of surface groups to pK_a = 2.5 and acidity to pH 1, so that pH − pK_a= −1.5. In this case, our theory predicts that colloidal surface charge density will be -3.2 mC/m^2. We then

https://doi.org/10.1021/acs.langmuir.2c02313
Langmuir 2022, 38, 13963−13971

change the intrinsic pK_a of surface groups to pK_a = 7.5 and pH 6, so that, again, pH − pK_a = −1.5. For this system, the theory predicts a surface charge density of −0.035 mC/m^2. Clearly both are different, even though both systems have pH − pK_a= −1.5. To confirm the predictions of the theory, we ran rMC simulations. The simulations yield surface charge densities of −2.9 mC/m^2 and −0.1 mC/m^2, for the two cases, respectively, in agreement with theory predictions. Clearly pH − pK_a is not a "universal" parameter, contrary to the claims made in ref 59.

Finally, we note that, within the present theory, the classical Henderson−Hasselbalch (HH) equation—much used in biochemistry and analytical chemistry to relate the value of pK_a with the pH when half the surface groups are protonated, p$H_{1/2}$—is modified to pK_a = p$H_{1/2}$ + $\beta q \varphi_{HH}$ log$_{10}$(e), where e is the Euler number and $\varphi_{HH} = \phi_0 + \phi_{dis} - \mu_{sol}$ is the electrostatic potential at the center of an adsorption site minus the electrostatic solvation free energy of a deprotonated site.

CONCLUSION

We have presented a theory that enables us to accurately calculate the surface charge of colloidal particles with uniformly distributed weak acid surface groups in solutions of various pH values and 1:1 electrolyte concentrations. The theory accounts for the shift of solution pH due to the presence of electrolyte. It also accounts self-consistently for the electrostatic potential produced by the discrete deprotonated surface groups. To examine the accuracy of the theory we have performed extensive rMC simulations, which show excellent agreement between theory and simulations for all system parameters explored in the present paper. We have also used the theory developed in the present paper to demonstrate that, contrary to recent suggestions,[59] pH − pK_a is not a universal parameter. The theoretical approach to account for discreteness and solvation effects introduced in the present paper can also be included within the MUltiSIte Complexation (MUSIC) model of Hiemstra et al.[66] used to study metal oxide surfaces; this will be the topic of future work.

Finally, it is well-known that multivalent ions, such as Ca^{2+}, interact strongly with carboxylate. In the future work we will attempt to extend the present theory to suspensions containing $CaCl_2$ salt. In that case, however, presence of multivalent ions will lead to electrostatic correlations even in the bulk electrolyte. This may require going beyond the PB equation and using classical density functional theory instead.

AUTHOR INFORMATION

Corresponding Authors

Amin Bakhshandeh − *Instituto de Física, Universidade Federal do Rio Grande do Sul, 91501-970 Porto Alegre, RS, Brazil;* orcid.org/0000-0001-5448-5179; Email: amin.bakhshandeh@ufrgs.br

Derek Frydel − *Department of Chemistry, Universidad Técnica Federico Santa María, 7820275 Santiago, Chile;* Email: derek.frydel@usm.cl

Yan Levin − *Instituto de Física, Universidade Federal do Rio Grande do Sul, 91501-970 Porto Alegre, RS, Brazil;* orcid.org/0000-0002-0636-7300; Email: levin@if.ufrgs.br

Complete contact information is available at: https://pubs.acs.org/10.1021/acs.langmuir.2c02313

Notes

The authors declare no competing financial interest.

ACKNOWLEDGMENTS

This work was partially supported by the CNPq, the CAPES, and the National Institute of Science and Technology Complex Fluids INCT-FCx. D.F. acknowledges financial support from the FONDECYT through Grant No. 1201192.

REFERENCES

(1) Butt, H.-J. A technique for measuring the force between a colloidal particle in water and a bubble. *J. Colloid Interface Sci.* **1994**, *166*, 109−117.

(2) Levin, Y. Electrostatic correlations: from plasma to biology. *Rep. Prog. Phys.* **2002**, *65*, 1577.

(3) Andelman, D.Introduction to electrostatics in soft and biological matter. In *Soft Condensed Matter Physics in Molecular and Cell Biology*; Scottish Graduate Series, Vol. *6*; Taylor and Francis, 2006.5997

(4) Borkovec, M.; Jönsson, B.; Koper, G. J. M. In *Surface and Colloid Science*; Matijević, E., Ed.; Springer US: Boston, MA, 2001; pp 99−339.

(5) Israelachvili, J. N.*Intermolecular and Surface Forces*; Academic Press, 2011.

(6) Vonarbourg, A.; Passirani, C.; Saulnier, P.; Benoit, J.-P. Parameters influencing the stealthiness of colloidal drug delivery systems. *Biomaterials* **2006**, *27*, 4356−4373.

(7) Everett, D. H.*Basic Principles of Colloid Science*; Royal Society of Chemistry, 2007.

(8) Russel, W. B., Saville, D. A., Schowalter, W. R.*Colloidal Dispersions*, 2nd Edition; Cambridge University Press: Cambridge, 1989.

(9) Mewis, J., Wagner, N. J.*Colloidal Suspension Rheology*, 1st Edition; Cambridge University Press: Cambridge, 2012.

(10) Dickinson, E.; Leser, M. E.*Food Colloids: Self-Assembly and Material Science*; Royal Society of Chemistry, 2007.

(11) Grahame, D. C. The electrical double layer and the theory of electrocapillarity. *Chem. Rev.* **1947**, *41*, 441−501.

(12) Guldbrand, L.; Jönsson, B.; Wennerström, H.; Linse, P. Electrical double layer forces. A Monte Carlo study. *J. Chem. Phys.* **1984**, *80*, 2221−2228.

(13) López-García, J.; Aranda-Rascón, M.; Horno, J. Electrical double layer around a spherical colloid particle: The excluded volume effect. *J. Colloid Interface Sci.* **2007**, *316*, 196−201.

(14) James, R. O.; Parks, G. A.*Surface and Colloid Science*; Springer, 1982; pp 119−216.

(15) Attard, P. Recent advances in the electric double layer in colloid science. *Curr. Opin. Colloid Interface Sci.* **2001**, *6*, 366−371.

(16) Carnie, S. L.; Chan, D. Y.; Gunning, J. S. Electrical double layer interaction between dissimilar spherical colloidal particles and between a sphere and a plate: The linearized poisson-boltzmann theory. *Langmuir* **1994**, *10*, 2993−3009.

(17) Krishnan, M. A simple model for electrical charge in globular macromolecules and linear polyelectrolytes in solution. *J. Chem. Phys.* **2017**, *146*, 205101.

(18) Hiemstra, T.; Van Riemsdijk, W. H. A surface structural approach to ion adsorption: the charge distribution (CD) model. *J. Colloid Interface Sci.* **1996**, *179*, 488−508.

(19) Hiemstra, T.; Venema, P.; Van Riemsdijk, W. H. Intrinsic proton affinity of reactive surface groups of metal (hydr) oxides: The bond valence principle. *J. Colloid Interface Sci.* **1996**, *184*, 680−692.

(20) Quesada-Pérez, M.; Callejas-Fernández, J.; Hidalgo-Alvarez, R. Interaction potentials, structural ordering and effective charges in dispersions of charged colloidal particles. *Adv. Colloid Interface Sci.* **2002**, *95*, 295−315.

(21) Fernandez-Nieves, A.; Fernandez-Barbero, A.; de Las Nieves, F.; Vincent, B. Ionic correlations in highly charge-asymmetric colloidal liquids. *J. Chem. Phys.* **2005**, *123*, 054905.

(22) Pianegonda, S.; Barbosa, M. C.; Levin, Y. Charge reversal of colloidal particles. *Europhys. Lett.* **2005**, *71*, 831.

(23) Guerrero-García, G. I.; González-Tovar, E.; de la Cruz, M. O. Effects of the ionic size-asymmetry around a charged nanoparticle: Unequal charge neutralization and electrostatic screening. *Soft Matter* **2010**, *6*, 2056−2065.
(24) Hermansson, M. The DLVO theory in microbial adhesion. *Colloids Surf., B* **1999**, *14*, 105−119.
(25) Ninham, B. W. On progress in forces since the DLVO theory. *Adv. Colloid Interface Sci.* **1999**, *83*, 1−17.
(26) Verwey, E. J. W. Theory of the Stability of Lyophobic Colloids. *J. Phys. Colloid Chem.* **1947**, *51*, 631−636.
(27) Boon, N.; Guerrero-García, G. I.; Van Roij, R.; De La Cruz, M. O. Effective charges and virial pressure of concentrated macroion solutions. *Proc. Natl. Acad. Sci. U. S. A.* **2015**, *112*, 9242−9246.
(28) Avni, Y.; Markovich, T.; Podgornik, R.; Andelman, D. Charge regulating macro-ions in salt solutions: screening properties and electrostatic interactions. *Soft Matter* **2018**, *14*, 6058−6069.
(29) Linderstrøm-Lang, K. Om proteinstoffernes ionisation. *C. R. Travaux Lab. Carlsberg* **1924**, *15*, 1−29.
(30) Ninham, B. W.; Parsegian, V. A. Electrostatic potential between surfaces bearing ionizable groups in ionic equilibrium with physiologic saline solution. *J. Theor. Biol.* **1971**, *31*, 405−428.
(31) Frydel, D. General theory of charge regulation within the Poisson-Boltzmann framework: Study of a sticky-charged wall model. *J. Chem. Phys.* **2019**, *150*, 194901.
(32) Podgornik, R. General theory of charge regulation and surface differential capacitance. *J. Chem. Phys.* **2018**, *149*, 104701.
(33) Avni, Y.; Andelman, D.; Podgornik, R. Charge regulation with fixed and mobile charged macromolecules. *Current Opinion in Electrochemistry* **2019**, *13*, 70−77. [Fundamental and Theoretical Electrochemistry Physical and Nanoelectrochemistry.]
(34) Markovich, T.; Andelman, D.; Podgornik, R. Charge regulation: A generalized boundary condition? *Europhys. Lett.* **2016**, *113*, 26004.
(35) Ong, G. M.; Gallegos, A.; Wu, J. Modeling Surface Charge Regulation of Colloidal Particles in Aqueous Solutions. *Langmuir* **2020**, *36*, 11918−11928.
(36) Curk, T.; Luijten, E. Charge Regulation Effects in Nanoparticle Self-Assembly. *Phys. Rev. Lett.* **2021**, *126*, 138003.
(37) Behjatian, A.; Walker-Gibbons, R.; Schekochihin, A. A.; Krishnan, M. Nonmonotonic Pair Potentials in the Interaction of Like-Charged Objects in Solution. *Langmuir* **2022**, *38*, 786−800.
(38) Bakhshandeh, A.; Frydel, D.; Levin, Y. Charge regulation of colloidal particles in aqueous solutions. *Phys. Chem. Chem. Phys.* **2020**, *22*, 24712−24728.
(39) Bakhshandeh, A.; Frydel, D.; Diehl, A.; Levin, Y. Charge Regulation of Colloidal Particles: Theory and Simulations. *Phys. Rev. Lett.* **2019**, *123*, 208004.
(40) Bakhshandeh, A.; dos Santos, A. P.; Levin, Y. Interaction between Charge-Regulated Metal Nanoparticles in an Electrolyte Solution. *J. Phys. Chem. B* **2020**, *124*, 11762−11770.
(41) Bakhshandeh, A.; Segala, M.; Escobar Colla, T. Equilibrium Conformations and Surface Charge Regulation of Spherical Polymer Brushes in Stretched Regimes. *Macromolecules* **2022**, *55*, 35−48.
(42) Parsons, D. F.; Salis, A. A thermodynamic correction to the theory of competitive chemisorption of ions at surface sites with nonelectrostatic physisorption. *J. Chem. Phys.* **2019**, *151*, 024701.
(43) Alexander, S.; Chaikin, P. M.; Grant, P.; Morales, G. J.; Pincus, P.; Hone, D. Charge renormalization, osmotic pressure, and bulk modulus of colloidal crystals: Theory. *J. Chem. Phys.* **1984**, *80*, 5776−5781.
(44) Aubouy, M.; Trizac, E.; Bocquet, L. Effective charge versus bare charge: an analytical estimate for colloids in the infinite dilution limit. *J. Phys. A: Math. Gen.* **2003**, *36*, 5835.
(45) Høye, J. S.; Lomba, E. Mean spherical approximation (MSA) for a simple model of electrolytes. I. Theoretical foundations and thermodynamics. *J. Chem. Phys.* **1988**, *88*, 5790−5797.
(46) Levin, Y.; Flores-Mena, J. E. Surface tension of strong electrolytes. *Europhys. Lett.* **2001**, *56*, 187−192.
(47) Güntelberg, E. Untersuchungen über Ioneninteraktion. *Z. Phys. Chem.* **1926**, *123*, 199−247.
(48) Gomez, D. A.; Frydel, D.; Levin, Y. Lattice-gas model of a charge regulated planar surface. *J. Chem. Phys.* **2021**, *154*, 074706.
(49) Levin, Y.; Arenzon, J. J. Why charges go to the surface: A generalized Thomson problem. *Europhys. Lett.* **2003**, *63*, 415.
(50) Thomson, J. J., XXIV. On the structure of the atom: an investigation of the stability and periods of oscillation of a number of corpuscles arranged at equal intervals around the circumference of a circle; with application of the results to the theory of atomic structure. *London, Edinburgh, Dublin Philos. Mag. J. Sci.* **1904**, *7*, 237−265.
(51) Pérez-Garrido, A.; Dodgson, M.; Moore, M. Influence of dislocations in thomson's problem. *Phys. Rev. B* **1997**, *56*, 3640.
(52) Bowick, M.; Cacciuto, A.; Nelson, D. R.; Travesset, A. Crystalline order on a sphere and the generalized Thomson problem. *Phys. Rev. Lett.* **2002**, *89*, 185502.
(53) Bausch, A. R.; Bowick, M. J.; Cacciuto, A.; Dinsmore, A. D.; Hsu, M. F.; Nelson, D. R.; Nikolaides, M. G.; Travesset, A.; Weitz, D. A. Grain Boundary Scars and Spherical Crystallography. *Science* **2003**, *299*, 1716−1718.
(54) Nishio, T. Monte Carlo simulations on potentiometric titration of cylindrical polyelectrolytes: Introduction of a method and its application to model systems without added salt. *Biophys. Chem.* **1994**, *49*, 201−214.
(55) Lunkad, R.; Barroso da Silva, F. L.; Košovan, P. Both Charge-Regulation and Charge-Patch Distribution Can Drive Adsorption on the Wrong Side of the Isoelectric Point. *J. Am. Chem. Soc.* **2022**, *144*, 1813−1825.
(56) Pasquali, S.; Frezza, E.; Barroso da Silva, F. L. Coarse-grained dynamic RNA titration simulations. *Interface Focus* **2019**, *9*, 20180066.
(57) Teixeira, A. A. R.; Lund, M.; Barroso da Silva, F. L. Fast Proton Titration Scheme for Multiscale Modeling of Protein Solutions. *J. Chem. Theory Comput.* **2010**, *6*, 3259−3266.
(58) Lund, M.; Åkesson, T.; Jönsson, B. Enhanced protein adsorption due to charge regulation. *Langmuir* **2005**, *21*, 8385−8388.
(59) Landsgesell, J.; Nová, L.; Rud, O.; Uhlík, F.; Sean, D.; Hebbeker, P.; Holm, C.; Košovan, P. Simulations of ionization equilibria in weak polyelectrolyte solutions and gels. *Soft Matter* **2019**, *15*, 1155−1185.
(60) Landsgesell, J.; Hebbeker, P.; Rud, O.; Lunkad, R.; Košovan, P.; Holm, C. Grand-reaction method for simulations of ionization equilibria coupled to ion partitioning. *Macromolecules* **2020**, *53*, 3007−3020.
(61) Stornes, M.; Blanco, P. M.; Dias, R. S. Polyelectrolyte-nanoparticle mutual charge regulation and its influence on their complexation. *Colloids Surf., A* **2021**, *628*, 127258.
(62) Bakhshandeh, A.; Frydel, D.; Levin, Y. Reactive Monte Carlo simulations for charge regulation of colloidal particles. *J. Chem. Phys.* **2022**, *156*, 014108.
(63) Bakhshandeh, A.; Levin, Y. Widom insertion method in simulations with Ewald summation. *J. Chem. Phys.* **2022**, *156*, 134110.
(64) Behrens, S. H.; Christl, D. I.; Emmerzael, R.; Schurtenberger, P.; Borkovec, M. Charging and aggregation properties of carboxyl latex particles: Experiments versus DLVO theory. *Langmuir* **2000**, *16*, 2566−2575.
(65) Kobayashi, M.; Skarba, M.; Galletto, P.; Cakara, D.; Borkovec, M. Effects of heat treatment on the aggregation and charging of Stöber-type silica. *J. Colloid Interface Sci.* **2005**, *292*, 139−147.
(66) Hiemstra, T.; Van Riemsdijk, W. H.; Bolt, G. Multisite proton adsorption modeling at the solid/solution interface of (hydr) oxides: A new approach: I. Model description and evaluation of intrinsic reaction constants. *J. Colloid Interface Sci.* **1989**, *133*, 91−104.

https://doi.org/10.1021/acs.langmuir.2c02313
Langmuir 2022, 38, 13963−13971